KINETIC STUDY OF THE THERMAL DEHYDRATION OF CALCIUM OXALATE MONOHYDRATE

YOSHIO MASUDA

Chemistry Division, General Education Department, Niigata University, Niigata 950-21 (Japan)

YOSHIO ITO, RYOKO ITO and KEIICHI IWATA

Department of Chemistry, Faculty of Science, Niigata University, Niigata 950-21 (Japan)

(Received 6 September 1985)

ABSTRACT

The kinetics of thermal dehydration of $CaC_2O_4 \cdot H_2O$ in static air and in a nitrogen flow were studied in detail by use of many accurate thermogravimetric (TG) data acquired on a microcomputer. This dehydration was apparently simple, but consisted of two processes: a two-dimensional phase boundary reaction (R_2) and a first-order reaction (F_1). The activation energies and pre-exponential factors were 119–189 kJ mol^{-1} and 1.12×10^{14}–4.57×10^{22} min^{-1} for the F_1 reaction, and 77.5–86.0 kJ mol^{-1} and 3.15×10^8–2.45×10^9 min^{-1} for the R_2 reaction, respectively. The R_2 reaction was the main process of the dehydration and seemed to consist of the elimination of water molecules. However, in the range of lower temperatures, dehydration was dominated by the F_1 reaction which seemed to consist of the external diffusion of water molecules eliminated from the surface of the specimen. In the present dehydration, the ability of reaction F_1 in the rate determination decreased with increasing temperatures because of the external diffusion activated. The thermal dehydration of $CaC_2O_4 \cdot H_2O$ was under the domination of reaction R_2 at temperatures above 391 K in nitrogen flow, and above 401 K in static air.

INTRODUCTION

Many methods have been proposed for the kinetic analysis of solid state reactions by thermogravimetry (TG) [1]. In these methods, the data to be analyzed are obtained from a TG curve on a recorder chart and processed with complicated calculations. Therefore, if a large number of accurate data are not available, a long time is consumed in analyzing them, and furthermore the results obtained cannot exactly describe the mechanism of the reaction. A microcomputer is effective in the acquisition of a large number of accurate TG data, and in the rapid and detailed analysis of the mechanism of thermal reaction of a solid.

In the present paper, a method is proposed to analyze the process of thermal decomposition of a solid by use of a microcomputer, from the above

point of view. The method was used to analyze the kinetics of thermal dehydration of $CaC_2O_4 \cdot H_2O$. The dehydration and decomposition of this compound have often been treated as a primary standard in the thermal analysis, and many reports have appeared on kinetic studies of its thermal dehydration [2–13]. Dollimore et al. [8] found that the rate of dehydration decreased sharply with an increase of water vapour pressure up to 0.0665 kN m^{-2} (0.5 mmHg), and at pressures beyond this value the rate increased from its minimum value to a slightly higher one, followed by a steady fall. Manche and Carroll [9] discerned a decrease in activation energy with the progress of dehydration. These findings suggest the complexity of the dehydration process. With these exceptions, many investigators concluded the dehydration process as a simple reaction, but the kinetic parameters and mechanisms reported by them were often different to each other.

It is worthwhile to analyze the kinetics of dehydration of $CaC_2O_4 \cdot H_2O$ with this method by use of many accurate TG data. It is expected that reliable new information concerning the dehydration mechanism will be obtained.

EXPERIMENTAL

Reagent

Calcium oxalate monohydrate of guaranteed grade (99.7%) was purchased. The specimen was sieved to a narrow fraction (250–300 mesh size) and dehydrated at 500 K for 2 days in an oven. The specimen of dehydrated CaC_2O_4 was placed in a desiccator saturated with H_2O vapor for a few days. The rehydrated oxalate was identified by means of IR spectrophotometry and thermogravimetry, then stored in a desiccator, and used without further purification.

Apparatus

Figure 1 is a block diagram of the experimental system which consists of a thermogravimetric apparatus and a microcomputer. The thermogravimetric system is a Shinku Riko TGD-5000 RH differential thermal microbalance. The voltages of output for the weight loss and the temperature of the specimen were amplified and acquired on a microcomputer (MZ-80C) via an AD converter (ICL 7109 modified in 13 bit). In this system, the AD converter was connected to the microcomputer by an analog multiplexer and an interface card (MZ-80I/0-1). A printer (MP-80) and an x–y plotter (WX-4675) were connected to the microcomputer.

When kinetic studies are based on thermogravimetry, two approaches are possible, viz. the dynamic method with rising temperature and the static
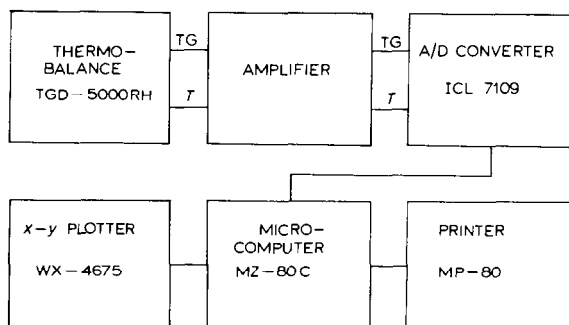
Fig. 1. Block diagram of the experimental system.

method at constant temperature. In this study, the former method was adopted.

Thermogravimetry was performed with heating rates of 2.5, 5, 8, 12, 16, and 20 K min^{-1}, in both static air and flowing nitrogen (99.99%) (flow rate, 50 cm^3 min^{-1}) atmospheres, by use of α-alumina as a reference material. In each measurement about 10 mg of specimen were weighed into a platinum crucible, and about 800 data concerning the weight loss were collected at regular intervals of time (Δt). The fraction dehydrated (α) was calculated from the TG data obtained. Temperatures (T) were recorded with an accuracy of ± 0.3 K. The rate of weight loss was reduced to ($\Delta\alpha/\Delta t$), where $\Delta\alpha$ is the difference between the values of the neighboring fractions dehydrated. Values of ($\Delta\alpha/\Delta t$) were calculated for a set of about 800 values of the dehydrating fractions and smoothed with the method of moving average of 25 terms.

Data analysis

Kinetic analysis of the TG data can be classified into two categories [1], namely differential and integral methods. In the present work, the TG data were analyzed on the basis of the modified Friedman's method [14,15] which is one of the differential methods.

The rate of weight loss during decomposition of a solid can be expressed by

$$d\alpha/dt = k\,f(\alpha) \tag{1}$$

where α is the decomposed fraction of solid after time t, k is the rate constant, and f(α) is a function depending on the decomposition mechanism. In the present analysis, the values of α ranging from 0.01 to 0.99 were selected from ~ 800 data with an interval of 0.01. Table 1 shows the f(α) functions used commonly for solid reactions [16]. The rate constant (k)

TABLE 1

Commonly used mathematical expressions of $f(\alpha)$ for solid reactions [16]

$f(\alpha)$	Symbol	Rate-controlling process
α^{-1}	D_1	One-dimensional diffusion
$[-\ln(1-\alpha)]^{-1}$	D_2	Two-dimensional diffusion
$[(1-\alpha)^{-1/3}-1]^{-1}(1-\alpha)^{1/3}$	D_3	Three-dimensional diffusion; Jander equation
$[(1-\alpha)^{-1/3}-1]^{-1}$	D_4	Three-dimensional diffusion; Ginstling–Brounshtein equation
$(1-\alpha)^{1/2}$	R_2	Two-dimensional phase boundary reaction
$(1-\alpha)^{1/3}$	R_3	Three-dimensional phase boundary reaction
$(1-\alpha)$	F_1	First-order reaction
$(1-\alpha)[-\ln(1-\alpha)]^{1/2}$	A_2	Random nucleation; Avrami equation I
$(1-\alpha)[-\ln(1-\alpha)]^{2/3}$	A_3	Random nucleation; Avrami equation II

depends on the absolute temperature (T) according to the Arrhenius equation

$$k = A \exp(-E/RT) \qquad (2)$$

where A, E and R are the pre-exponential factor, activation energy and gas constant, respectively. If the temperature increases linearly with time, the heating rate (β) can be expressed by eqn. (3)

$$\beta = dT/dt \qquad (3)$$

Equations (1), (2), and (3) are combined to eliminate k

$$(d\alpha/dT)\beta = A \exp(-E/RT)f(\alpha) \qquad (4)$$
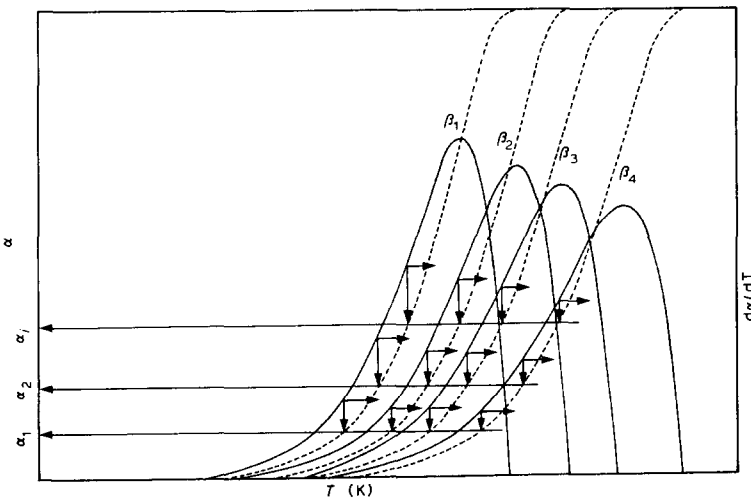

Fig. 2. Graphs for obtaining $(d\alpha/dT)\beta$ and T for each α. ($\cdots\cdots$) Decomposed fraction (α) and (———) $d\alpha/dT$, at various heating rates (β).
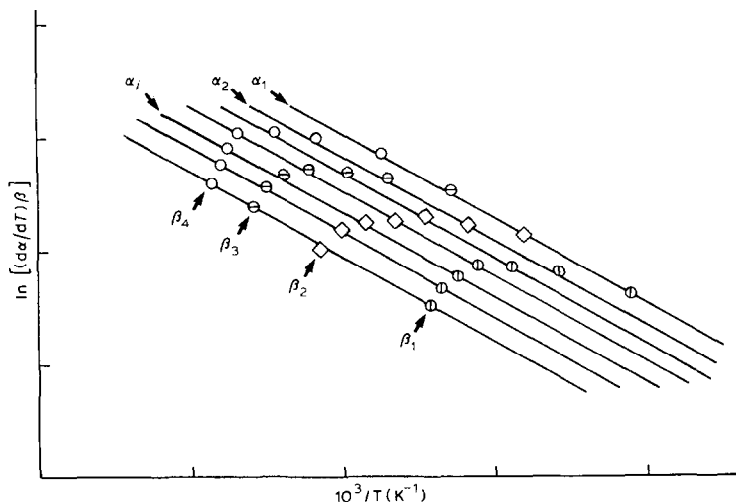
Fig. 3. Plots of $\ln[(d\alpha/dT)\beta]$ vs. $1/T$ for the data from Fig. 2.

The logarithmic form of eqn. (4) is

$$\ln[(d\alpha/dT)\beta] = \ln A + \ln f(\alpha) - E/RT \tag{5}$$

For each α, the values of $[(d\alpha/dT)\beta]$ and T can be determined from the TG and the differential thermogravimetric (DTG) curves obtained at various heating rates, as shown in Fig. 2. The plot of $\ln[(d\alpha/dT)\beta]$ vs. $1/T$ gives a straight line as shown in Fig. 3. The value of E can be determined from its slope, while the intercept of the line gives the value of $\ln A + \ln f(\alpha)$. If the activation energy scarcely varies with the progress of reaction, the difference in value of intercepts of neighboring lines is given by

$$\ln[(d\alpha_{i+1}/dT)\beta] - \ln[(d\alpha_i/dT)\beta] = \ln f(\alpha_{i+1}) - \ln f(\alpha_i) \tag{6}$$

The values of $\ln[(d\alpha_{i+1}/dT)\beta] - \ln[(d\alpha_i/dT)\beta]$ obtained from experiments can be compared with the calculated values of $\ln f(\alpha_{i+1}) - \ln f(\alpha_i)$ for various reaction mechanisms shown in Table 1, in order to determine the most reasonable $f(\alpha)$ function. When the experimental values of $(d\alpha/dT)\beta$, E, and $f(\alpha)$ are substituted in eqn. (5), the value of A can be determined.

The above procedures were programmed on the microcomputer and applied to the kinetic analysis of the thermal dehydration of $CaC_2O_4 \cdot H_2O$.

RESULTS AND DISCUSSION

Figure 4 shows the typical TG and differential thermal analysis (DTA) curves obtained in a static air atmosphere. The smoothness of the curve suggests that dehydration proceeds through a one-step reaction as reported
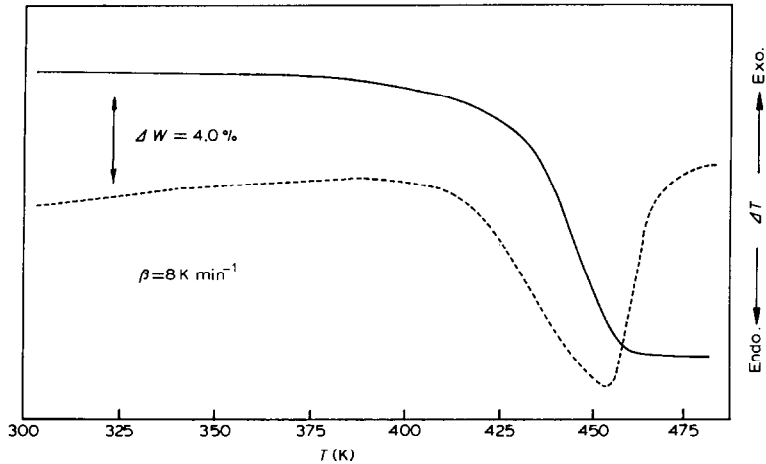
Fig. 4. Typical TG (———) and DTA (— — —) curves for the thermal dehydration of $CaC_2O_4 \cdot H_2O$ in static air.

by many authors [2–7,10–12]. Plots of $\ln[(d\alpha/dT)\beta]$ vs. $1/T$ give straight lines, as shown in Fig. 5. Two different groups of parallel lines could be clearly recognized in the regions $0.04 \leqslant \alpha \leqslant 0.08$ and $0.75 \leqslant \alpha \leqslant 0.95$, and the values of their activation energies were 189 and 86.0 kJ mol^{-1}, respectively.
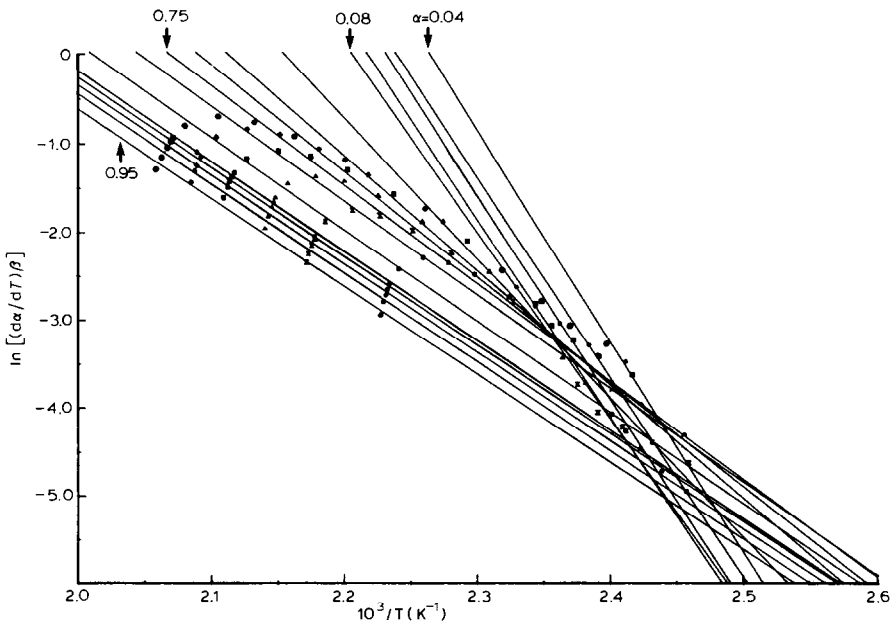

Fig. 5. Plots of $\ln[(d\alpha/dT)\beta]$ vs. $1/T$ for each α of thermal dehydration of $CaC_2O_4 \cdot H_2O$ in static air.
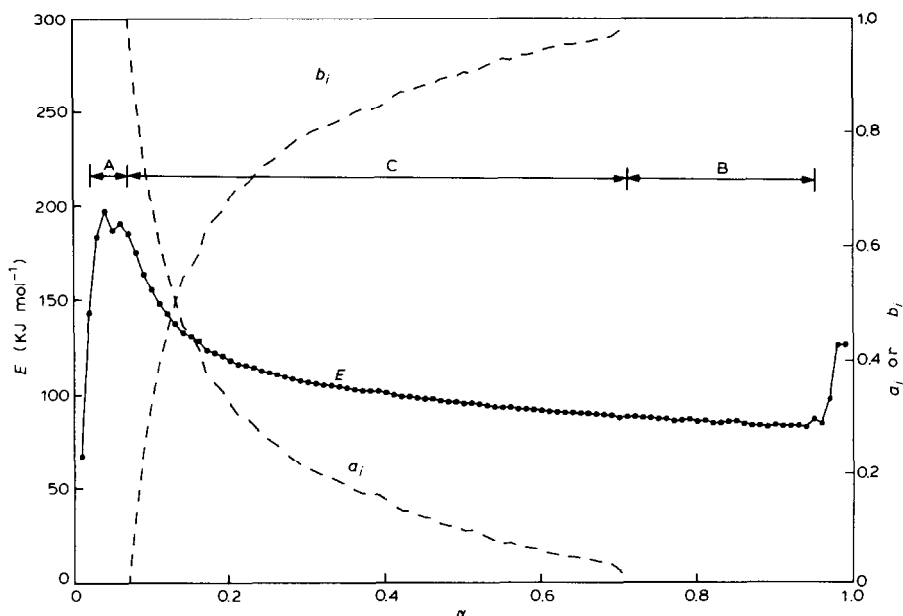
Fig. 6. Relation between activation energy (E) and dehydrating fraction (α). a_i and b_i are the weights of reactions I and II, respectively, at each E_i value.

These findings indicate that the dehydration, being apparently simple, consists of at least two independent reactions (I and II) whose mechanisms were determined as follows: the rates of these two reactions can be described by equations (7) and (8)

$$(d\alpha_1/dT)\beta = A_1 \exp(-E_1/RT)f(\alpha_1) \quad \text{for reaction (I)} \tag{7}$$

$$(d\alpha_2/dT)\beta = A_2 \exp(-E_2/RT)f(\alpha_2) \quad \text{for reaction (II)} \tag{8}$$

Figure 6 shows the relation between E and α. If reaction (I) alone takes place in region A in Fig. 6 and reaction (II) alone in region B, the predominant process of dehydration varies from reactions (I) to (II) in region C. The activation energy (E_i) for each α_i in region C can be expressed by eqn. (9)

$$E_i = a_i E_1 + b_i E_2 \tag{9}$$

where coefficients a_i and b_i represent the weight of reactions (I) and (II), respectively, and satisfy eqn. (10)

$$a_i + b_i = 1 \tag{10}$$

In Fig. 6, a_i and b_i, calculated by use of eqns. (9) and (10), are shown. The values of a_i and b_i obtained were employed to determine the new fractions,

TABLE 2

Results of analysis of the thermal dehydration of $CaC_2O_4 \cdot H_2O$ in a static air and in flowing N_2 atmospheres

f(α)	In static air		In flowing N_2	
	F_1	R_2	F_1	R_2
α-range [a]	0.03–0.75	0.07–0.95	0.03–0.58	0.07–0.95
E (kJ mol^{-1})	189	86.0	119	77.5
A (min^{-1})	4.57×10^{22}	2.45×10^9	1.12×10^{14}	3.15×10^8
Proportion (%) [b]	19.7	80.3	23.7	76.3

[a] α-range shows the region in which each reaction takes place.
[b] Proportion shows the ratio of each reaction to a whole dehydration.

$\alpha_{1,i}$ and $\alpha_{2,i}$ for reactions (I) and (II), respectively

$$\alpha_{1,i} = \sum_{i=1}^{i} a_i \bigg/ \sum_{i=1}^{total} a_i \tag{11}$$

$$\alpha_{2,i} = \sum_{i=1}^{i} b_i \bigg/ \sum_{i=1}^{total} b_i \tag{12}$$

The values of $[(d\alpha_{j,i}/dT)\beta]$ for reaction j were calculated by use of these new fractions, $\alpha_{j,i}$. For each reaction, the function, $f_j(\alpha_i)$, and the pre-exponential factor, A_j, were estimated by use of eqns. (5) and (6) from the values of $\alpha_{j,i}$, E_j, and $[(d\alpha_{j,i}/dT)\beta]$ obtained.

The results are shown in Table 2. Reaction (I) has characteristics of a first-order reaction (F_1), and reaction (II) is a two-dimensional phase boundary reaction (R_2) which is the predominant process for the dehydration (about 80% of the whole reaction). If these two reactions take place successively, they may be associated with the formation of an intermediate hydrate. So, X-ray diffraction analysis was carried out on the original oxalate monohydrate and on the specimens heated to 393, 408, 418, 428, 438, 453, and 483 K. However, no intermediate hydrate could be found. Therefore, these two reactions seemed not to occur consecutively.

Further, the TG data were obtained in a flowing nitrogen atmosphere and analyzed according to the same method in order to discuss the mechanism of the reaction in detail. Table 2 shows a comparison with the results in static air. In flowing nitrogen atmosphere, the kinetic behavior of the dehydration was similar to that in static air. The kinetic parameters (E and A) for reaction R_2 were of approximately similar order as those obtained in static air, whereas the kinetic parameters for reaction F_1 were smaller in magnitude than those found in static air. The rate constants, k_1 and k_2, calculated for the F_1 and R_2 reactions, respectively, in flowing nitrogen, tend to be larger than those found in static air, as shown in Table 3. The ratios $k_1(N_2)/k_1$

TABLE 3

The rate constants, k_1 and k_2, calculated for the reactions F_1 and R_2 at various temperatures, respectively

Rate constant (min^{-1}) [a]	Temperature (K)					
	373	383	393	403	413	423
k_1 (air)	1.55×10^{-4}	7.63×10^{-4}	3.46×10^{-3}	1.45×10^{-2}	5.69×10^{-2}	2.09×10^{-1}
k_2 (air)	2.21×10^{-3}	4.57×10^{-3}	9.08×10^{-3}	1.75×10^{-2}	3.25×10^{-2}	5.87×10^{-2}
k_1 (N_2)	2.42×10^{-3}	6.59×10^{-3}	1.71×10^{-2}	4.21×10^{-2}	9.95×10^{-2}	2.26×10^{-1}
k_2 (N_2)	4.41×10^{-3}	8.48×10^{-3}	1.57×10^{-2}	2.84×10^{-2}	4.97×10^{-2}	8.47×10^{-2}

[a] Air and N_2 in parentheses indicate that the dehydrations were carried out in static air and in flowing N_2 atmospheres, respectively.

(air) and $k_2(N_2)/k_2$ (air) decreased with increasing temperature as shown in Table 4. This tendency is more remarkable for reaction F_1. The above facts indicate that reaction F_1 is more affected by the surrounding atmosphere than reaction R_2.

It is also noticeable that the value of k_2 is larger than that of k_1 at lower temperatures (Table 3). This suggests that reaction F_1 is the rate-determining step at lower temperatures in the present dehydration. However, this relationship between k_1 and k_2 is reversed at 406 K for the experiment in static air, and at 391 K in flowing nitrogen. The reversing temperature is clearly recognized on the typical DTG dehydration curve: the DTG curves sharply accelerate at 406 K for the experiment in static air and at 391 K in flowing nitrogen, as shown in Fig. 7.

These findings can be interpreted on the basis of the following assumptions: the two-dimensional phase boundary reaction (R_2) is related to the elimination of water molecules in the specimen, and the first-order reaction (F_1) to external diffusion of the eliminated water molecules from the surface of the specimen particles.

TABLE 4

The ratios of k_1 $(N_2)/k_1$ (air) and k_2 $(N_2)/k_2$ (air) at various temperatures [a]

Ratio	Temperature (K)								
	373	383	393	403	413	423	433	443	453
$\dfrac{k_1\ (N_2)}{k_1\ (air)}$	15.5	8.64	4.94	2.90	1.75	–	–	–	–
$\dfrac{k_2\ (N_2)}{k_2\ (air)}$	–	–	1.73	1.63	1.53	1.44	1.36	1.29	1.23

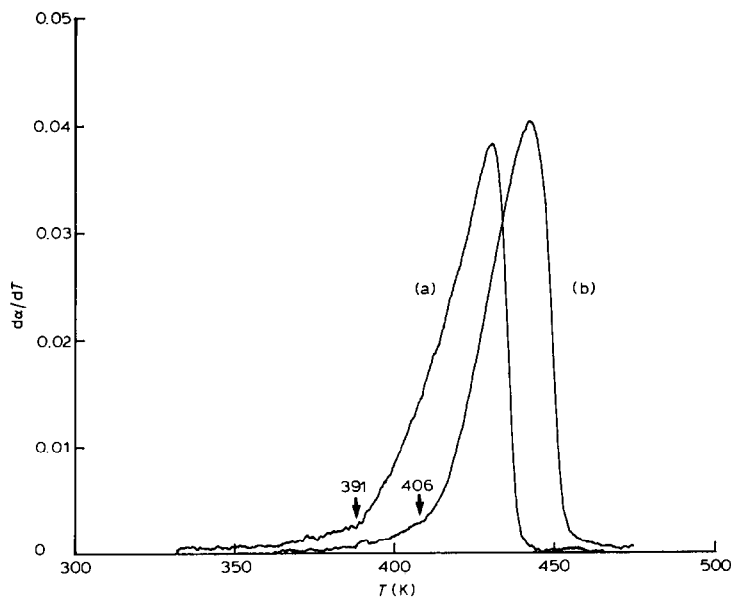[a] N_2 and air in parentheses indicate dehydrations in flowing N_2 and in static air, respectively.

Fig. 7. Typical DTG curves obtained at a heating rate of 2.5 K min^{-1} for the thermal dehydration of $CaC_2O_4 \cdot H_2O$ (a) in flowing N_2 and (b) in static air.

It is reasonable that the step of elimination of water molecules is not influenced directly by the experimental atmosphere, whereas the external diffusion of eliminated water molecules must depend on it. Since the eliminated water molecules are removed quickly from the surface of a solid in a flowing nitrogen, the rate of external diffusion increases more than that in static air.

It is known that in the phase boundary reaction the diffusion of the reactant or product takes place rapidly, so the rate of the overall reaction is exclusively determined by the chemical process occurring at the reactant–product interface [17]. However, in the dehydration of $CaC_2O_4 \cdot H_2O$, external diffusion of the eliminated water molecules seemed to be the rate-determining step, especially at low temperatures. Consequently, the first-order reaction seemed to proceed as the initial step of dehydration, especially at low temperatures. On the other hand, the dehydration showed a natural characteristic of the phase boundary reaction at higher temperatures where the eliminated water molecules diffused rapidly from the surface.

REFERENCES

1 W.E. Brown, D. Dollimore and A.K. Gallway, in C.H. Bamford and C.F.H. Tipper (Ed.), Comprehensive Chemical Kinetics, Vol. 22, Reactions in the Solid State, Elsevier, Amsterdam, 1980, p. 97.
2 E.S. Freeman and B. Carroll, J. Phys. Chem., 62 (1958) 394.
3 H.H. Horowitz and G. Metzger, Anal. Chem., 35 (1963) 1464.
4 A.W. Coats and J.P. Redfern, Nature (London), 201 (1964) 68.
5 P.K. Chatterjee, J. Polym. Sci., Part A, 3 (1965) 4253.
6 F. Škvára and V. Šatava, J. Therm. Anal., 2 (1970) 325.
7 J. Mu and D.D. Perlmutter, Thermochim. Acta, 49 (1981) 207.
8 D. Dollimore, T.E. Jones and P. Spooner, J. Chem. Soc. A, (1970) 2809.
9 E.P. Manche and B. Carroll, Thermochim. Acta, 24 (1978) 1.
10 H.G. Weidemann and A.V. Tets, Naturwissenschaften, 54 (1967) 442.
11 H.M. Hauser and J.E. Field, Thermochim. Acta, 27 (1978) 1.
12 S. Gurrierri, G. Siracusa and R. Cali, J. Therm. Anal., 6 (1974) 293.
13 K.N. Ninan and C.G.R. Nair, Thermochim. Acta, 30 (1979) 25.
14 H.L. Friedman, J. Polym. Sci. Polym. Chem. Ed., 6 (1964) 183.
15 S. Tanabe and R. Otsuka, Netsusokutei, 4 (1977) 139.
16 J.H. Sharp, G.W. Brindley and B.N.N. Achar, J. Am. Ceram. Soc., 49 (1966) 379.
17 S.F. Hulbert, J. Br. Ceram. Soc., 6 (1969) 11.